Jour. Korean Inst. Mining Geol.
V. 17, No. 2, 1984, p. 101-107

Analyses of Apparent Resistivity Responses from Near-Surface Cavities

Hee Joon Kim*

Abstact : This paper describes dipole-dipole apparent resistivity responses from near-surface cavities in otherwise homogeneous earth materials. In applying the dipole-dipole resistivity method to the problem of locating and delineating subsurface cavities, it is important to know apparent resistivity responses not only for conductive bodies but also for resistive ones. Dipole-dipole apparent resistivities for these bodies are calculated by the numerical modeling technique using an integral equation solution.

The magnitude and pattern of apparent resistivity is highly dependent on the ratio of body resistivity to background resistivity. In conductive bodies, the largest anomaly of apparent resistivity appears at the outside of the body. In resistive bodies, however, the position of the largest anomaly coincides with the location of the body. The field results gathered at Okinawa, Japan in 1978 showed that peak anomalies occurred at the locations of air-filled cavities.

Introduction

In these days, near-surface cavities become a serious problem in civil engineering. However, mainly due to the complexity of near-surface layers, it is usually difficult to detect the cavities by conventional explorations such as the seismic and magnetic surveys.

The widespread application of the electrical resistivity method as primary exploration tools, coupled with developments in rapid and accurate data acquisition techniques, warrants more quantitative interpretation of the geologic stucture than is currently practiced. Induced polarization (IP) equipments, for example, enable us to apply the dipole-dipole array to the resistivity survey in many field environments because of its accurate and powerful data acquisition ability (Takeuchi et al., 1983). In this paper we analyze dipole-dipole apparent resistivity responses from the near-surface cavities in otherwise homogeneous earth materials.

In the resistivity method we have been usually interested in conductive targets such as mineral deposits and goethermal resources. The resistivity of subsurface cavity, however, varies with its contents. Water-filled cavities usually indicate conductive responses but air-filled cavities indicate resistive ones. Therefore, in applying the resistivity method to the problem of locating and delineating these cavities, it is important to kuow the apparent resistivity responses not only for conductive targets but also resistive ones.

In this paper we stndy first the effect of the resistivity ratio between target and background on the dipole-dipole apparent resistivity responses. These responses are calculated by the three-dimensional integral equation method (Kim, 1983). Next, as an example of resistive targets, we interpret the field results for air-filled cavity exploration gathered at Okinawa, Japan in 1978.

* Department of Applied Geology, National Fisheries University of Pusan, Pusan 608, Korea.

Fundamental equation and models

A typical integral equation for inhomogeneities with uniform resistivities was developed by Snyder (1976). In the case of a simple body characterized by uniform resistivity ρ_2 in an otherwise uniform half-space of resistivity ρ_1, using an appropriate Green's function G, a potential ϕ is given by

$$\phi(\boldsymbol{r}, \boldsymbol{r}_S) = \frac{\rho_1 I}{4\pi} G(\boldsymbol{r}, \boldsymbol{r}_S) + \frac{1}{4\pi} \iint_S q(\boldsymbol{r}') G(\boldsymbol{r}, \boldsymbol{r}') dS' \quad (1)$$

where

$$q=2\frac{\rho_2-\rho_1}{\rho_2+\rho_1}\boldsymbol{n}\cdot\nabla\phi, \qquad (2)$$

$\boldsymbol{r}$ is the field point, $\boldsymbol{r}_S$ the position of pole source, $\boldsymbol{r}'$ the position of surface elements ds', I the strength of current source located at the point $\boldsymbol{r}_S$, q the surface charge density of inhomogeneity, and $\boldsymbol{n}$ the outward unit vector normal to the boundary surface S. The Green's function for the half-space is

$$G(\boldsymbol{r},\ \boldsymbol{r}')=\frac{1}{|\boldsymbol{r}-\boldsymbol{r}'|}+\frac{1}{|\boldsymbol{r}-\boldsymbol{r}''|} \qquad (3)$$

where $\boldsymbol{r}''$ is the reflected point of $\boldsymbol{r}'$ across the half-space boundary. Applying the method of moments (Harrington, 1968), equation (1) is solved numerically (e.g., Endo et al., 1979).

To illustrate the effects of the resistvity ratio, ρ_2/ρ_1, on the apparent resistivity responses, we select two different models as shown in Figs. 1 and 2. One model (Fig. 1) has a cubic body which is two units (dipole length) on a side. The depth to the top of the body is one unit. The cublc body consists of eight small cubic cells, and each cell has one unit on a side. The other model (Fig. 2) has a dipping body which is inclined 20 degrees against the earth's surface. The depth to the top of the body is one unit, and the strike length is two units, The dipping body consists of forty cubic cells, and each cell has one half unit on a side.

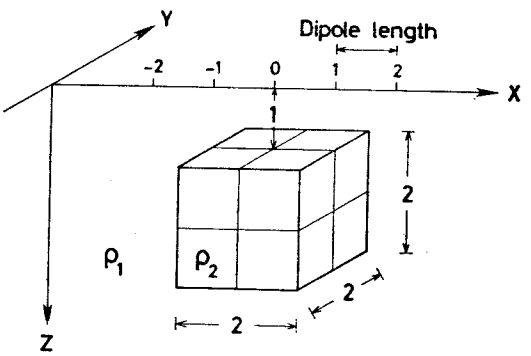

Fig. 1 Cubic model. The earth except for a cubic body of resistivity ρ_2 is taken to be a half-space of resistivity ρ_1. The size of the body is 2×2×2 units (dipole length), and the depth to the top of the body is one unit.

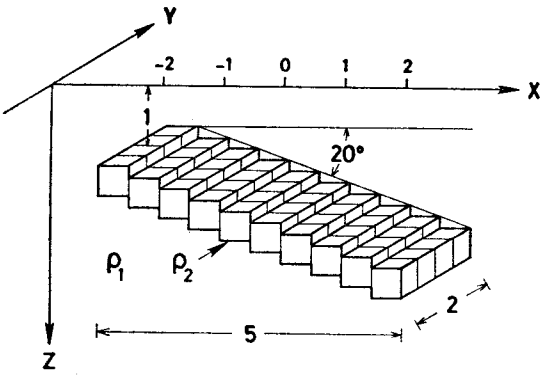

Fig. 2 Dipping model. The earth except for a dipping body of resistivity ρ_2 is taken to be a half-space of resistivity ρ_1. The body inclines 20 degrees against the earth's surface (X-Y plane). The depth to the top of the body is one unit of dipole length, the strike length is two units and the total width is five units.

Only the dipole-dipole array is considered here because the dipole-dipole array usually gives the largest anomalies and has best overall resolution (Coggon, 1973; Takeuchi et al., 1983). Numerical results are shown as a function of the normalized apparent resistivity: ρ_a/ρ_1, where ρ_a is the calculated apparent resistivity. The results are illustrated by pseudosectional views, and these plotting points are shown in Fig. 3. All profile lines shown in this paper are perpendicular to the strike of each body.

Numerical results

Fig. 4 shows dipole-dipole apparent resistivity responses of the cubic body for four resistivity ratios: $\rho_2/\rho_1=1/16$, 1/4, 4 and 16. The most remarkable feature is that the position of the largest anomaly (the lowest or highest apparent resistivity) varies with the resistivity ratio. For the conductive bodies ($\rho_2/\rho_1=$ 1/16 and 1/4), the lowest apparent resistivities appear at the both outsides of the bodies. For the resistive bodies ($\rho_2/\rho_1=$ 4 and 16), on the other hand, the highest responses occur at the centers of the bodies. Therefore the patterns of anomaly between the conductive and the resistive bodies are different.

Fig. 5 shows apparent resistivities at the points

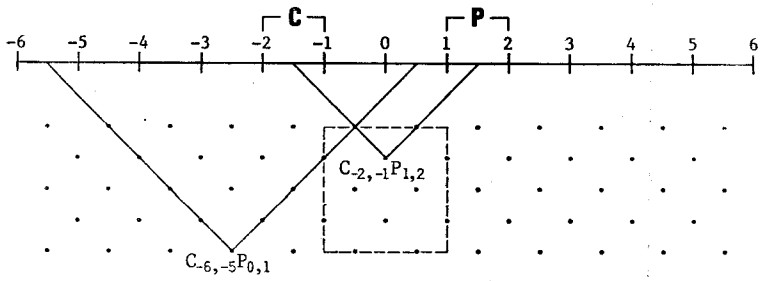

Fig. 3 Relation of plotting points to current and potential dipoles in the dipole-dipole array. C and P represent the current and potential dipoles, respectively.

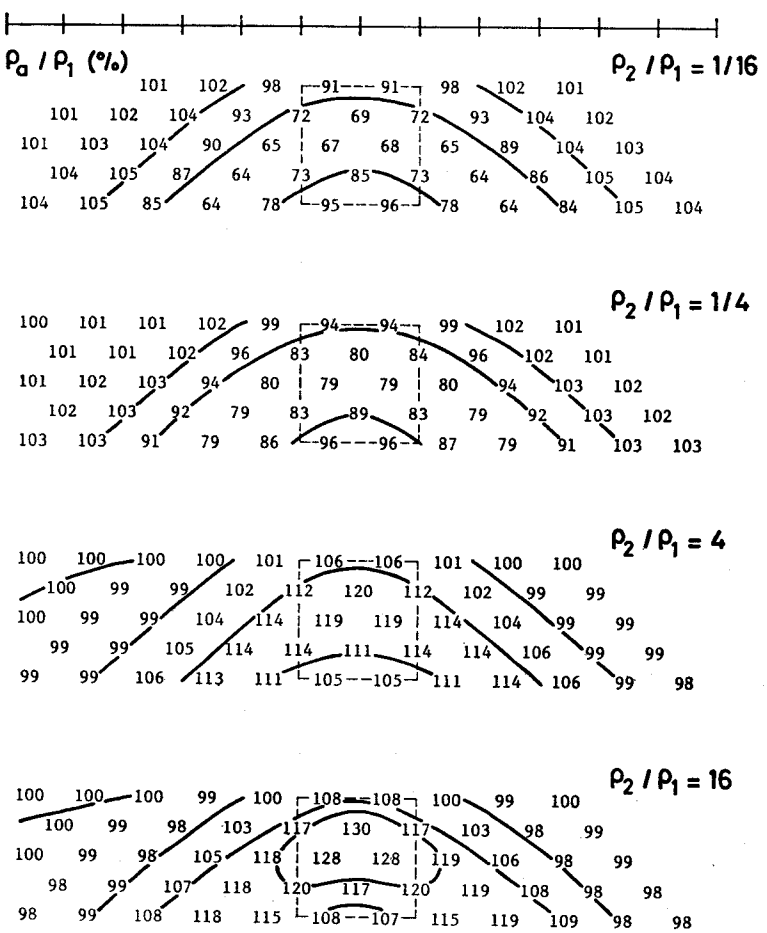

Fig. 4 Effect of resistivity ratio (ρ_2/ρ_1=1/16, 1/4, 4 and 16) on apparent resistivity responses for the cubic model.

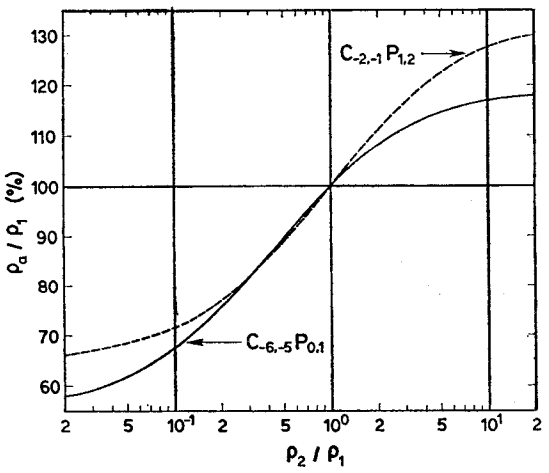

Fig. 5 Apparent resistivity curves at the points of $C_{-2,-1}$ $P_{1,2}$ and $C_{-6,-5}P_{0,1}$ (see Fig. 3) for the cubic model.

of $C_{-2,-1}$ $P_{1,2}$ and $C_{-6,-5}$, $P_{0,1}$(see Fig. 3) with the highest and lowest apparent resistivities, respectively (Fig. 4). For the resistive case with $\rho_2/\rho_1 > 1$, $C_{-2,-1}$ $P_{1,2}$ has the maximum anomaly (highest value) in the pseudo-section. For the strongly conductive case with $\rho_2/\rho_1 \leq 0.2$, however, the maximum anomaly (lowest value) occurs at $C_{-6,-5}$ $P_{0,1}$, and its symmetrical point of $C_{-1,0}$, $P_{5,6}$, For the intermediate case, weakly condctive case, the maximum anomaly usually moves to the other point. Hence anomaly patterns are divided into three cases: resistive, weakly conductive and strongly conductive. The weakly conductive case is transitional between the strongly conductive and the resistive cases. The pseudo-section for $\rho_2/\rho_1 = 1/4$ in Fig. 4 is an expamle of such transitional case, and relatively broad and low-amplitude anomalies appear around the body.

Fig. 6 compares apparent resistivity responses of the dipping body for the same resistivity ratios as in Fig. 4. The patterns of anomaly change dramatically with resistivity ratios. For the strongly conductive body ($\rho_2/\rho_1 = 1/16$), the largest anomaly appears on the side opposite to the direction of dip, while for the resistive budies ($\rho_2/\rho_1 = 4$ and 16) the largest anomalies are in the direction of dip. On the other hand, for the weakly condutive body ($\rho_2\rho_1 = 1/4$), the anomaly pattern is neraly symmetrical in spite of the asymmetrical body, If we ignore the magnitude of apparent resistivity, the anomaly for the conductive dipping body is almost similar to that for the weakly conductive cubic body.

In the interpretation of field data, interpreters usually pay attention to the position of the largest anomaly or the pattern of anomaly. Results of Figs. 4 and 6 suggest that, for strongly conductive targets such as mineral deposits or geothermal resources, the largest dipole-dipole anomaly does not coincide with the location of target, and sophisticated interpretation techniques are needed. Drillings would be unsuccessful if the hole were spotted over the largest anomaly. For weakly conduetive targerts such as water-filled cavities, it would be impossible to delineate the shape of target by the pattern analysis alone. For resistive targets such as air-filled cavities or tunnels, on the other hand, it would be relatively easy to predict the location and/or shape of target on the basis of the largest anomaly and/or the anomaly pattern in the field data. In the following section, as an example of such resistive cases, we present two results of field survey aimed at delineating subsurface air-filled cavities.

Field results

The field survey was carried out on an area of limestone containing air-filled cavities at Okinawa, Japan in 1978 (Ooba, 1979). The purpose of this survey was to predict the cavities shallower than about 10 m. We measured the dipole-dipole apparent resistivity by using an IP equipment.

Figs. 7 and 8 show the field result which detect two cavities in the limestone area of Okinawa. In these figures, since the resistivity of air-filled cavity seems to be infinite, over 500 $\Omega \cdot$m can be regarded as anomalies associated with the cavity.

When we compare the field results with the

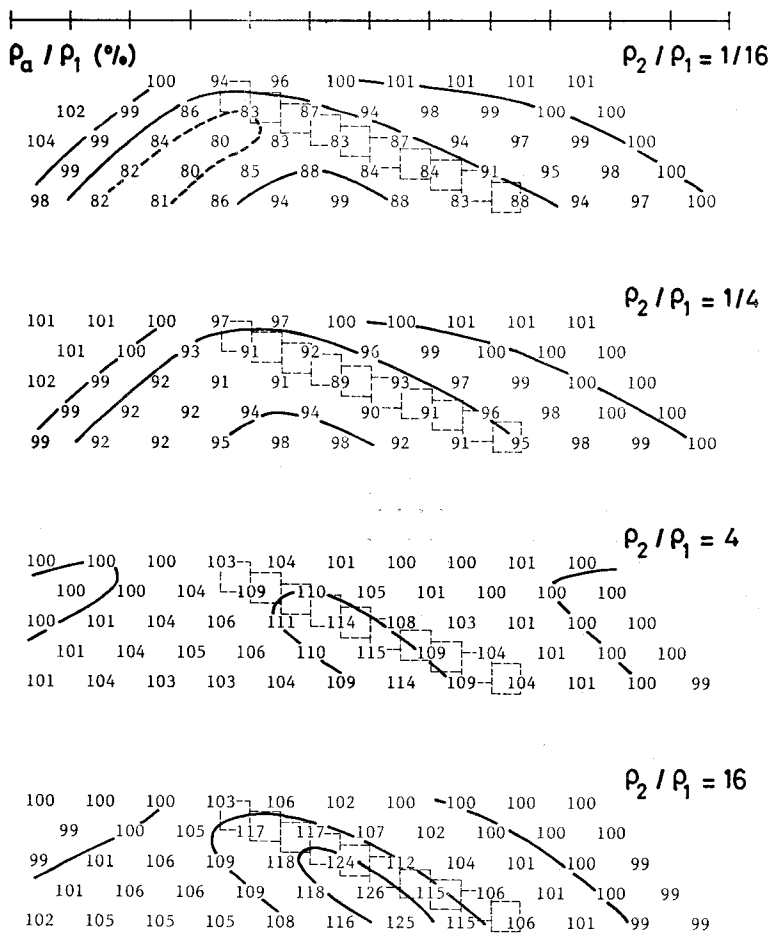

Fig. 6 Effect of resistivity ratio (ρ_2/ρ_1=1/16, 1/4, 4 and 16) on apparent resistivity responses for the dipping model.

numerical ones, it is found that the patterns of anomaly in Figs. 7 and 8 are nearly similar to those in Figs. 4 and 6 (ρ_2/ρ_1=16), respectively. As a first approximation, therefore, the shapes of the cavities are roughly estimated to be the model shapes.

The existence of the cavities in Fig. 7 was actually confirmed by a simple drilling. Its drilling point selected at just above the highest apparent resistivity. The cavity in Fig. 8 was also confirmed by entering into the cavity.

Discussion and conclusions

In the foundamental integral equation, the resistivity ratio enters into the from $(\rho_2-\rho_1)/(\rho_2+\rho_1)$ (sse equation (2)). For an extreme case, i.e., perfectly conductive or resistive body,

$$\frac{\rho_2-\rho_1}{\rho_2+\rho_1}=\begin{cases}-1: \text{perfect conductor}\\ +1: \text{perfect resistor.}\end{cases}$$

This shows that further decrease or increase in the resistivity ratio in Figs. 4, 5 and 6 will have little effects on apparent resistivities. The result

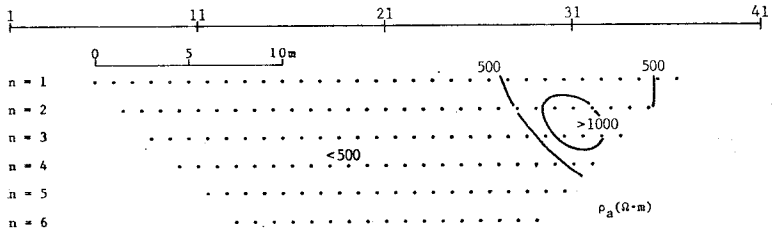

Fig. 7 Dipole–dipole apparent resistivities obtained at a limestone area of Okinawa, Japan in 1978. The length of line is 40 m. An air-filled cavity exists at 2 or 3m depth below the electrode No. 31.

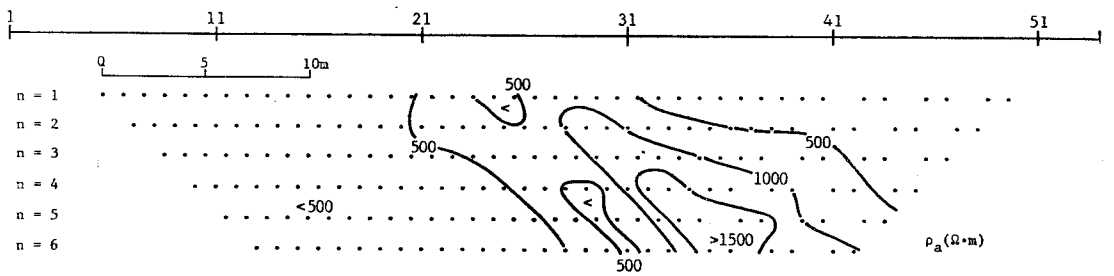

Fig. 8 Dipole–dipole apparent resistivities obtained at a limestone area of Okinawa, Japan in 1978. The length of line is 53 m. An air-filled cavity exists at more than 4 m depth below the electrode No. 35.

for a perfect resistor is given by Spiegel et al. (1980).

Dipole-dipole apparent resistivity anomalies are highly dependent on the resistivity ratio. The resistivity ratio affects not only the magnitude of the anomalies but also the pattern of those. In strongly condutive cases, the peak value appears at the outside of body. Due to this fact the selection of drilling points will be difficult in actual field situation. Note that, even in this case, if the thickness of body is larger than the width, the peak dipole-dipole anomaly occurs at the location of body (Yoshizumi and Irie, 1967).

In weakly conductive cases, relatively broad and low-amplitude anomalies appear around the bodies. The dipping body produces a symmetrical anomaly pattern, and its pattern is almost similar to that of the cubic body. Hence the prediction of target shape will be difficult by the pattern analysis alone. However, since the main objective of field survey is usually to deduce the location of target, such difficulty may not be a serious problem.

In resistive cases, on the other hand, the largest anomaly occurs at the location of target, and the anoamaly pattern is clearly distinguished from the target. This fact will make the wide application of dipole-dipole resistivity survey in many fields. In the survey of civil engineering or archaeology, for example, the resistivities of targets such as cavities or tombs are usually higher than those of surrounding media.

The dipole-dipole field survey carried out at Okinawa, Japan in 1978 successfully found the subsurface air-filled cavity. Its position and shape were predicted by the largest anomaly and the anomaly pattern. The array comparison for cavity exploration is given by Takeuchi et. al. (1983).

Acknowledgments

This work has been supported by the research grant of 1983 from the Ministry of Education, the Republic of Korea; this support is gratefully acknowledged.

References

Coggon, J. H. (1973) A comparison of IP electrode arrays. Geophysics, v. 38, No. 4, p. 737—761.

Endo, G., Y. Yamamoto, M. Takeuchi and K. Noguchi (1979) On the numerical calculation method using an integral equation solution (I), Butsuri-Tanko, v. 32, No. 3, p, 117—125. (in Japanese)

Harrington, R. F. (1968) Field Computation by Moment Methods. New York, Macmillan Co., 229p.

Kim, H. J. (1983) Three-dimensional standard curves in induced polarization method. Jour. Korean Inst. Mining Geol, v. 16, No. 4, p. 269-276

Ooba, T. (1979) Detection of cavity. Geotechnics, v. 11, 97—99. (in Japanese)

Snyder, D. D. (1976) A method for modeling the resistivity and IP response of two-dimensional bodies. Geophysics. v. 51, No. 5, p. 997—1015.

Spiegel, R. J., V. R. Sturdivant and T. E. Owen (1980) Modeling resistivity anomalies from localized voids under irregular terrain. Geophysics, v. 45, No. 7, p. 1164—1193.

Takeuchi, M., H. J. Kim, K. Noguchi and G. Endo (1983) Near-surface surveys with resistivity method. Comparison of electrode arrays, Butsuri-Tanko, v. 36, No. 3, p. 111—117. (in Japanese)

Yoshizumi, E. and T. Irie (1967) Variation of resistivity curves due to electrode configurations. Butsuri-Tanko, v. 20, No. 5, p. 208—212. (in Japanese)

지하천부의 공동에 의한 외견 비저항의 해석

김 희 준*

요약 : 쌍극자 배치 사용시 지하천부에 존재하는 공동으로 인한 외견 비저항을 해석하였다. 쌍극자 배치를 사용한 비저항법을 이용하여 지하공동의 위치나 모양을 밝히는 데는 전도성 물체뿐만이 아니라 저항성 물체에 대한 외견 비저항 반응을 알아야 한다. 이들 물체에 대한 외견 비저항은 적분방정식을 이용한 수치계산 방법으로 구하였다.

외견 비저항의 크기와 패턴은 물체와 주위 비저항의 비율에 따라서 크게 달라진다. 전도성 물체의 경우 최대이상은 물체의 바깥쪽에 나타나지만, 저항성 물체의 경우 최대이상의 출현위치는 물체의 위치와 일치한다. 후자의 예로서 1978년 일본 오끼나와에서 실시한 야외조사에서 최대이상이 공동의 위치에 나타나는 것이 확인되었다.

*부산수산대학 응용지질학과